Chapman, Daniel S. 2013. **Greater phenological sensitivity to temperature on higher Scottish mountains: new insights from remote sensing**. *Global Change Biology*, 19 (11). 3463-3471. 10.1111/gcb.12254

Title Greater phenological sensitivity to temperature on higher Scottish mountains: new insights from remote sensing

Running head Elevational gradients in mountain phenology

Authors Daniel S. Chapman[1]

[1] NERC Centre for Ecology & Hydrology, Bush Estate, Edinburgh EH26 0QB, UK

Corresponding author Daniel Chapman, tel. +44 131 4458549, fax +44 131 4453943, e-mail dcha@ceh.ac.uk

Keywords Alpine vegetation, climate change, ecosystem phenology, satellite monitoring, NDVI, EVI, MODIS.

Type of paper Primary research article

Abstract

Mountain plants are considered among the species most vulnerable to climate change, especially at high latitudes where there is little potential for poleward or uphill dispersal. Satellite monitoring can reveal spatio-temporal variation in vegetation activity, offering a largely unexploited potential for studying responses of montane ecosystems to temperature and predicting phenological shifts driven by climate change. Here, a novel remote sensing phenology approach is developed that advances existing techniques by considering variation in vegetation activity across the whole year, rather than just focusing on event dates (e.g. start and end of season). Time series of two vegetation indices (NDVI and EVI) were obtained from the MODIS satellite for 2786 Scottish mountain summits (600-1344 m elevation) in the years 2000-2011. NDVI and EVI time series were temporally interpolated to derive values on the first day of each month, for comparison with gridded monthly temperatures from the preceding period. These were regressed against temperature in the previous months, elevation and their interaction, showing significant variation in temperature sensitivity between months. Warm years were associated with high NDVI and EVI in spring and summer, while there was little effect of temperature in autumn and a negative effect in winter. Elevation was shown to mediate phenological change via a magnification of temperature responses on the highest mountains. Together, these predict that climate change will drive substantial changes in mountain summit phenology, especially by advancing spring growth at high elevations. The phenological plasticity underlying these temperature responses may allow long-lived alpine plants to acclimate to warmer temperatures. Conversely, longer growing seasons may facilitate colonisation and competitive exclusion by species currently restricted to lower elevations. In either case, these results show previously unreported seasonal and elevational variation in the temperature sensitivity of mountain vegetation activity.

Introduction

Changes to species' phenology (the seasonality of ecological processes) and their aggregate effects at ecosystem levels are among the clearest documented impacts of recent rapid climate change (Cleland *et al.*, 2007, Walther *et al.*, 2002). Across a large range of taxa, a general pattern of phenological shifting in response to warming has emerged, with advancing early and mid-season events (leafing, flowering and fruiting) and less predictable but often delayed late-season events (leaf senescence) (Menzel *et al.*, 2006, Thackeray *et al.*, 2010). Large-scale coherent phenological shifts could have many important consequences. Altered synchrony of intra- or interspecific interactions may affect individual fitness and population dynamics (Miller-Rushing *et al.*, 2010). Longer growing season lengths are likely to relax constraints on species distributions, promote range expansion and drive changes in community composition (Morin *et al.*, 2008). At the ecosystem level, altered seasonality of respiration and photosynthesis is affecting the global carbon cycle (Keeling *et al.*, 1996). Therefore, understanding phenological shifts and predicting future trajectories of change are very important goals for ecological research.

This is perhaps especially true in mountain ecosystems where growing seasons are short and sharply demarcated by cold winters (Körner, 2003). Many studies emphasise that dates of mountain plant spring growth and flowering respond to temperature and other climate-related drivers such as snow cover (Aldridge *et al.*, 2011, Inouye *et al.*, 2002, Totland & Alatalo, 2002, Wipf & Rixen, 2010). Although it seems clear that warming is affecting the timing of these individual events, a broader consideration of how climatic variation affects phenology of the whole vegetation community across the whole of the year, and how this varies geographically, e.g. with elevation, is lacking. Recently, uphill migration of low-elevation species and large changes in species richness on mountain summits have been associated with warming (Gottfried *et al.*, 2012, Pauli *et al.*, 2012). Because these changes in species

composition are likely facilitated by longer growing seasons and may lead to different phenological patterns at the community scale, there is strong motivation for assessing the current-day link between temperature and phenology on mountain summits, and using this to predict future vegetation phenology.

Remote sensing of vegetation activity may provide a standardised avenue for enquiry into mountain phenology across multiple years and locations (Pettorelli *et al.*, 2005, Qiu *et al.*, 2012). Satellites including MODIS (Moderate Resolution Imaging Spectroradiometer) provide vegetation indices (VI) such as the normalised difference VI (NDVI) and enhanced VI (EVI) at reasonably high spatial and temporal resolutions (Huete *et al.*, 2002). NDVI correlates well with vegetation productivity so is useful for characterising the phenology of vegetation activity. EVI provides complementary information but suffers less from atmospheric and soil effects and is more strongly related to vegetation canopy cover, especially in high biomass environments such as forests (Huete *et al.*, 2002). Traditionally, phenology studies have processed time series of remote sensed VIs to compute calendar day-based estimates of phenological events, such as dates of green-up, peak growth, and senescence (Pettorelli *et al.*, 2005, Wu & Liu, 2012). This approach has demonstrated trends for earlier and longer growing seasons at continental scales (Stöckli & Vidale, 2004). However, a weakness of the method is that the temporal resolutions of VI time series are generally orders of magnitude greater than typical known rates of change in event dates (< 1 day per year; Menzel *et al.*, 2006, Thackeray *et al.*, 2010). Furthermore, phenological studies would benefit from considering the full seasonal activity pattern of the focal species or ecosystem, rather than just the dates of a small set of events (Hodgson *et al.*, 2011, Post *et al.*, 2008).

In this study, a novel technique for analysing phenological change from VI time series is used to assess elevational patterns of vegetation seasonality and their sensitivity to temperature on

the summits of 2766 mountains in Scotland. Instead of estimating phenology event dates, the full seasonal pattern of VI variation is considered. To achieve this, temporal interpolation with regression splines is used to approximate VI values on fixed days, chosen here to fall on the first day of each month for congruence with monthly temperature data. Each month's first-day VIs are analysed against mean temperatures in the preceding months to assess their climatic sensitivity. Between-month variation in temperature sensitivity allows the forecasting of shifts in the VI phenology curves (at monthly resolution) for climate change scenarios. The analysis also considers interactions between temperature and elevation to test the hypothesis that phenological change in montane ecosystems is mediated by elevation.

Materials and Methods

Study area and data sources

The location and elevation of every mountain summit (hill top ≥600 m above sea level) in Scotland were extracted from the Database of British and Irish Hills (Jackson *et al.*, 2012) (Fig. 1). The database contained 2857 such summits, with a maximum elevation of 1344 m. Of these 91 were excluded as having a higher peak within 354 m, meaning they may share the same 250x250 m MODIS pixel (see below). Summits were used in the study as a way of roughly standardising topography, compared to using pixels from slopes of varying aspect. In Scotland, 600 m is generally interpreted as being the upper limit of the tree line, 900m is the upper limit of the sub-alpine zone and 1200 m is the upper limit of the low-alpine zone (Coll *et al.*, 2010). The climate is highly oceanic (especially in the west) with intermittent snow cover during winter, except on the highest mountains.

Remote-sensed data from the 250x250 m and 16-day MOD13Q1 composite product of the MODIS satellite (NASA Land Processes Distributed Active Archive Center, 2013) were acquired for each summit between day 49 in 2000 (the earliest date at which MODIS data are available – other satellites provide earlier NDVI but at much coarser resolution) to the end of 2012. Two VIs (NDVI and EVI) were extracted from MOD13Q1. These are normalised to a nadir view and standard solar angular geometry using the bidirectional reflectance distribution function of each pixel (Huete *et al.*, 2002). As a result, seasonal variation in view and solar zenith angles of the MODIS satellite will not affect the seasonal pattern of VI variation. Also obtained from MOD13Q1 were a data quality flag and the exact acquisition days for each 16-day compositing period (Huete *et al.*, 2002). The data quality flag indicates whether the satellite had a clear view of the land or was observing snow or cloud.

As a variable to investigate climatic effects on vegetation phenology, regional monthly gridded mean temperatures up to the end of 2011 were obtained from the CRU TS3.2 dataset (University of East Anglia Climatic Research Unit, 2012) at a resolution of 0.5° longitude and latitude (Fig. 1). From CRU TS3.2, mean temperatures for the whole region (not the summits) in February and July were 1.9 °C and 12.8 °C, respectively, over the period of study. Even though temperature data were only available to the end of 2011, MODIS VI data were obtained up to the end of 2012, to avoid edge effects in the phenological modelling (see below).

Pre-processing of the MODIS VI data

Before phenological analysis, I identified and removed unreliable VI observations from the data. First, the data quality flag was used to exclude snow and cloud observations, because they obscure the vegetation (Fig. 2a). Some of the remaining observations were also considered unreliable because of inaccuracy in sensor calibration, atmospheric correction and cloud and snow masking (Huete *et al.*, 2002, Pettorelli *et al.*, 2005). These were identified as being outliers from the long-term average seasonal VI trend, after flagged snow and cloud were removed. Seasonal VI trends were estimated by fitting circular cubic regression splines with the 'mgcv' R package (Wood, 2003) where VI is modelled as a function of the day of the year (Fig. 2b). The circular nature of the spline ensured a seamless wrapping of the seasonal curve. Spline smoothness is controlled by the number of degrees of freedom, of which I allowed five. Outliers were classified from the residuals of the spline if they were outside of the range $[Q_1-(Q_3-Q_1), Q_3+(Q_3-Q_1)]$ where Q_1 and Q_3 are the first and third quartiles of the residuals (Chambers *et al.*, 1983). Most outliers were negative residuals (i.e. unusually low VI observations), reflecting the downwards biasing of VI measures by atmospheric contamination (Pettorelli *et al.*, 2005, Zhang *et al.*, 2003). Because large negative residuals will affect least squares fitting, two iterations of the spline and outlier

identification algorithm were applied, with the second iteration being performed on the subset of data remaining after the first (Fig. 2b).

Interpolation of first-of-month VI

Because the temperature data were monthly, first-of-month VI values were estimated by a temporal interpolation, where data permitted. After exclusion of cloud, snow and outliers, non-circular cubic regression splines were fitted to the multi-year time series (Hodgson *et al.*, 2011) with mgcv (Wood, 2003) (Fig. 2c). To represent seasonal oscillations, splines were specified with 65 degrees of freedom (five per year). Interpolated VI values from the spline curve were calculated for the first day of each month between 2000 and 2011, for use as response variables in the modelling of temperature effects on VI. To ensure interpolation was reliable, I did not interpolate first-of-month VI if fewer than three valid VI observations were within ±30 days of the first-of-month day (Fig. 2c).

Analysis of VI variation

Bayesian generalised linear mixed models (GLMMs) were used to test the sensitivity of interpolated first-of-month NDVI and EVI in each calendar month to variation in mean temperature of the previous months. The GLMMs for each month were specified to contain fixed effects of temperature, elevation ($\log_{10}$-transformed to improve conformance to normality, see Fig. 1 inset) and their interaction. A random effect of the summit identity was included to account for repeat sampling from the same mountains and to accommodate the difference between the average temperature in the CRU TS3.2 grid cell and that experienced on the mountain summit.

Separate models were fitted for each month of the year, since it may be expected that all fixed and random effects may vary seasonally. Theoretically, it may have been possible to fit a

single model in which month interacted with all fixed and random effects, but I found it simpler and more tractable to work with a set of monthly models. Models were also fitted with alternative temperature variables, based on means over the previous one to six months. The optimal temperature averaging period was selected based on minimising the summed deviance information criteria (DIC) of the GLMMs for each of the 12 months.

GLMMs were estimated through a Bayesian procedure using the Markov Chain Monte Carlo (MCMC) algorithm as implemented by the R package 'MCMCglmm' (Hadfield, 2010) to sample from the posterior distributions. GLMMs were specified with a Gaussian error structure, uninformative priors, burn-in of 3,000 MCMC iterations followed by 500,000 iterations to sample posterior distributions with a thinning interval of 10 iterations. More iterations were not used because of computational effort and the large number of individual models to fit. From the fixed effect posterior samples, I calculated posterior means, 95% highest posterior density (HPD) intervals and two-tailed *P* values (twice the proportion of the posterior sample that was of opposite sign to the posterior mean). Fixed effect pseudo-R^2 values were calculated from the squared correlation between the observed VIs and values calculated from the posterior mean fixed effects (i.e. ignoring variation explained by the random effect).

Projection of VI in the 2050s

To illustrate the potential for future climate change to drive shifts in ecosystem phenology, I used monthly mean temperatures predicted for the 2050s by the HadCM3 climate model (Johns *et al.*, 2003) assuming three SRES emissions scenarios (A1b, A2a and B2). The A scenarios project less effort to reduce greenhouse gas emissions than the B scenario, while the '1' scenarios assume greater globalisation than the '2' scenarios. HadCM3 projections in the 2050s for these scenarios were obtained at a 1/24° resolution and were aggregated to the

CRU TS3.2 grid by taking means. Compared to observed annual mean temperatures from 2000-2011, the model predicts that by the 2050s the annual mean temperature of the study region will warm by an average of 1.4 °C for A1b, 0.3 °C for A2a and 0.1 °C for B2. However summer warming is projected to be greater (for July 2.1 °C, 0.8 °C and 0.7 °C respectively). To estimate potential phenological shifts driven by these temperature changes, the posterior mean fixed effects of the GLMMs developed above were used to calculate first-of-month VI profiles for the 2050s temperatures. These were contrasted with the current-day first-of-month VI profiles calculated from the 2000-2011 temperatures.

Results

Pre-processing and temporal interpolation

An example of the pre-processing and interpolation for NDVI is shown in Fig. 2. Across all summits, the median percentage of MODIS observations excluded because of cloud or snow was 32.5% (95^{th} percentile range = 17.2-58.1%). Both cloud and snow cover were more prevalent at higher elevations (Pearson's r = 0.798 and 0.697, respectively, both $P < 0.001$). The percentages of non-obscured MODIS observations identified as outliers from the long-term average seasonal VI curves (probably representing undiagnosed problems with sensor calibration, instrument noise, atmospheric correction or cloud and snow masking) were 18.7% for NDVI (95^{th} percentile range = 8.8-26.5%) and 15.1% for EVI (95^{th} percentile range = 4.6-24.2%). There were weak but significant tendencies for fewer outliers to be identified on the higher summits (r = -0.188 for NDVI and r = -0.303 for EVI, both $P < 0.001$). After exclusion of cloud, snow and outliers, the long-term average seasonal VI curves (Fig. 3) showed a clear seasonal oscillation indicating that they are useful for phenological studies. The average seasonal patterns were more asymmetrical for NDVI than EVI. Both VIs were also depressed at higher elevations, probably because of reduced vegetation productivity and cover. However, the timing of the average phenological peaks was not noticeably affected by elevation (Fig. 3).

According to the data quality criteria established in the Materials and Methods, spline interpolation of first-of-month VIs (Fig. 2c-d) was possible in 38.2% of cases for NDVI and 40.7% for EVI, giving respective sample sizes for the subsequent analyses of 153,879 and 162,763. Because of greater cloud and snow cover, there was a strong decline in the proportion of months where interpolation was possible with increasing elevation (r = -0.766 for NDVI and r = -0.732 for EVI, both $P < 0.001$) and more interpolations were possible in

summer than in winter (Fig. 4). Nevertheless reasonable sample sizes for analysis were obtained throughout the year at elevations below 1100 m (Fig. 4).

VI sensitivity to temperature

Bayesian GLMMs were fitted separately for each calendar month and VI to model interpolated first-of-month values as a function of interactions between regional mean temperature in the previous months and elevation. Comparing models for average temperatures over the previous one to six months, the strongest temperature effect (lowest DIC) was obtained by averaging over three months (ΔDIC > 200 for all alternative averaging windows). Overall pseudo-R^2 values calculated from the posterior mean fixed effects (i.e. ignoring variation explained by the random effects) were 0.562 for NDVI and 0.402 for EVI. Mean pseudo-R^2s for individual months were 0.233 for NDVI (range 0.138-0.325) and 0.120 for EVI (range 0.036-0.251), in both cases peaking in March and being lowest in December and January.

Samples from the GLMM fixed effect posterior distributions showed that elevation had a significant ($P < 0.05$) negative effect on VI in 21 of 24 cases (see Table S1). Temperature main effects were statistically significant in 17 cases, and there were significant interactions between temperature and elevation in 19 cases (Table S1). As shown in Fig. 5, these interactions exhibited a strong coherence in temperature sensitivity between months, which was not specified in the models fitted independently for each calendar month. At the lowest elevations, first-of-month VIs were relatively insensitive to temperature but exhibited small positive effects during spring and summer (Fig. 5). At higher elevations, there were strong positive effects of warm temperature in spring and summer, peaking on 1st May. There was also a strong negative association between high temperatures and VIs in winter (1st December

to 1st March) at high elevations. These patterns did not qualitatively depend on the choice of a 3-month temperature averaging window (Fig. S1).

Modelled future phenological shifts

VIs predicted for the projected mean temperatures in the 2050s under emissions scenario A1b substantially differed from those observed in 2000-2011 (Fig. 6). Warming was predicted to drive reductions in VI during winter (1st December to 1st March) and increase VI in spring and summer (especially on 1st May and 1st June) with the greatest changes predicted for the higher summits. The large increases in spring VI and slight increase in late summer can reasonably be interpreted as leading to an earlier and longer growing season (though I did not attempt to estimate season start and end days). The highest summits also increased in phenological amplitude (difference between maximum and minimum VI). Qualitatively similar results were obtained for two other emissions scenarios (A2a and B2; see Figs. S2 and 3), though these predict less warming in Scotland and so the changes were smaller.

Discussion

This study is the first to quantify large-scale elevational gradients in the sensitivity of phenology to climate in alpine ecosystems. Because alpine species cannot readily disperse to track the shifting climate space, especially in Scotland where there is no currently-unvegetated nival belt to colonise, gaining a better understanding of how montane ecosystems and species respond to climate change is very important for their conservation. This analysis of two complementary remote-sensed vegetation indices shows that over the past decade, warmer years have been associated with increased vegetation activity in spring and summer, little change in autumn, and reduced activity in winter. This signals a temperature-driven phenological shift towards earlier and longer growing seasons with increased phenological amplitude. Furthermore, the analysis demonstrates that climatic effects on phenology are mediated by elevation, with more pronounced temperature sensitivity on higher summits than at the lower end of the alpine zone.

The finding that warm years are associated with earlier green-up of the vegetation (increased VI in spring months) mirrors conclusions from multi-species meta-analyses (Menzel *et al.*, 2006, Thackeray *et al.*, 2010), studies of individual montane plants (Aldridge *et al.*, 2011, Inouye *et al.*, 2002, Totland & Alatalo, 2002, Wipf & Rixen, 2010) and patterns found for start-of-spring indicators inferred from remote sensing (Fisher *et al.*, 2006, Stöckli & Vidale, 2004). However, this analysis considers temperature effects on the full seasonal pattern of vegetation activity and not just dates for specific phenological events. Between-month differences in temperature sensitivity (Figs. 5 and 6) show that the advance in the early growing season occurs via a fairly uniform leftwards shifting of the phenology curve during spring and early summer (April to July), without much change to the pattern of senescence in autumn. The lack of temperature sensitivity towards the end of the growing season perhaps reflects photoperiodic controls on senescence, which may be adapted to pre-empt winter

frosts (Körner, 2003). Predictions for the 2050s (Fig. 6) suggest that at the resolution of this study (months) the timing of the phenological peak will not change because of warming. However, based on the projected changes it seems likely that a sub-month advance in the peak would occur, especially at higher elevations and for EVI (Fig. 6).

The seasonal pattern of temperature sensitivity uncovered in the analysis is consistent with the majority of individuals and species opportunistically starting to grow earlier and then maintaining activity for longer during warm years. If only a small subset of species responded in this way, then the VI phenology curve would retain the same peak, but be increasingly skewed to the left rather than uniformly shifted. If all species started to grow earlier but also senesced earlier, the whole curve and its peak would shift to the left. If only a subset of species did this, then the curve would form a secondary bimodal early-season peak, as has been observed for sub-alpine flowering phenology (Aldridge *et al.*, 2011). This argument highlights the increased understanding of phenological change that can be gained from studying the whole seasonal curve rather than just the dates of selected events (Hodgson *et al.*, 2011, Post *et al.*, 2008).

An interesting and previously unreported pattern arising from this study was a negative association between high temperature and both VIs in winter (December to March), which was again significantly greater at high elevations. This effect is large enough for climate change to potentially cause large decreases in winter VI on the highest summits (Fig. 6). I suggest that this result should be accepted with caution as the sample size of valid observations in winter and at high elevations was low (Fig. 4). Furthermore, if warmer winters allowed observation of summits normally covered in snow and these had lower winter VIs than those summits with less snow cover, then it is possible that a spurious negative correlation between temperature and VI may have been introduced. However, a plausible biological explanation is that in the oceanic climate of Scotland, mild periods in

winter will melt lying snow and encourage premature carbohydrate mobilisation and plant growth when there is still a risk of frost damage (Crawford, 2000) which could reduce VI. Unfortunately I was unable to investigate snowmelt effects on VI explicitly in this analysis because snowmelt was estimated very imprecisely from the snow cover flag due to cloud cover and the coarse temporal resolution of the data. Nevertheless, the results suggest that winter temperature rises could play an important role in Scottish alpine species' and community responses to warming. Impacts of winter climate change are less commonly studied than those of summer warming and so I suggest further studies, including snow removal (Wipf & Rixen, 2010) and artificial warming (Saavedra *et al.*, 2003) experiments, should explicitly test this on Scotland's oceanic mountains.

The statistical models of first-of-month VI were used to project future changes in vegetation phenology curves for climate change scenarios. The greatest change was predicted for the higher hills, consistent with the previously discussed elevational variation in temperature sensitivity. There was no way to test whether the models were capable of predicting long-term phenological change, as has been done for single-species models (Hodgson *et al.*, 2011), so these projections should also be accepted with caution. There are at least two reasons why the use of recent responses to climate may not accurately predict the long-term trajectory of change. First, the analysis conflates within-population (i.e. temporal) and between-population (i.e. spatial) effects of temperature. Sophisticated analyses beyond the scope of this paper are required to separate robustly both components of temperature responses and their interactions with elevation (Phillimore *et al.*, 2012). However, individual summits did vary considerably between years in line with regional temperatures (Fig. S4) indicating significant within-summit temporal responses to annual meteorological variation. Second, in the long-term the plant community at a given elevation may well come to resemble that currently found at lower elevations because of uphill species migration (Gottfried *et al.*, 2012). Phenological

responses currently observed at high elevation, may therefore become similar to those currently observed on lower summits. The results here suggest that for Scottish mountains, this may reduce phenological sensitivity to temperature at high elevations. This emphasises a need to integrate modelling species and community distributions with that of phenology (Morin *et al.*, 2008) to make robust predictions of the impact of climate change on vegetation phenology.

Montane plants tend to be slow-growing and long-lived, so low temporal turnover might be expected in their populations and communities. As such, between-year phenological change in response to temperature may indicate a high degree of phenotypic plasticity among alpine plants. Phenological plasticity could enhance the resilience of alpine ecosystems to climate change, especially if replicated across other demographic traits (Doak & Morris, 2010). Nevertheless, recent re-surveys have shown that over roughly the same period as this study, species richness on Scottish mountain summits has increased (Pauli *et al.*, 2012) through 'thermophilization' (i.e. uphill migration; Gottfried *et al.*, 2012). Indeed, of 17 European mountain ranges assessed, Scotland's mountains experienced the greatest thermophilization and the second greatest summer temperature increase (Gottfried *et al.*, 2012). The strong links between temperature, elevation and vegetation phenology demonstrated here suggest a causal link between phenological change and community change. Earlier and longer potential growing seasons may facilitate uphill expansion of sub-alpine species and the altered community composition may then affect the pattern of vegetation phenology. This two-way feedback suggests a complex pattern of responses to climate change in alpine ecosystems. Future studies should explore the implications of this for species persistence during a period of rapid global change.

Acknowledgements

This work was funded under the NERC CEH Science Budget. I am grateful for helpful discussions with France Gerard and the comments of two anonymous referees.

References

Aldridge G, Inouye DW, Forrest JRK, Barr WA, Miller-Rushing AJ (2011) Emergence of a mid-season period of low floral resources in a montane meadow ecosystem associated with climate change. *Journal of Ecology*, **99**, 905-913.

Chambers JM, Cleveland WS, Kleiner B, Tukey PA (1983) *Graphical Methods for Data Analysis,* Belmont, CA., Wadsworth International Group.

Cleland EE, Chuine I, Menzel A, Mooney HA, Schwartz MD (2007) Shifting plant phenology in response to global change. *Trends in Ecology & Evolution,* **22**, 357-365.

Coll J, Gibb SW, Price MF, Mcclatchey J, Harrison J (2010) Developing site scale projections of climate change in the Scottish Highlands. *Climate Research,* **45**, 71-85.

Crawford RMM (2000) Tansley Review No. 114. Ecological hazards of oceanic environments. *New Phytologist,* **147**, 257-281.

Doak DF, Morris WF (2010) Demographic compensation and tipping points in climate-induced range shifts. *Nature,* **467**, 959-962.

Fisher JI, Mustard JF, Vadeboncoeur MA (2006) Green leaf phenology at Landsat resolution: Scaling from the field to the satellite. *Remote Sensing of Environment,* **100**, 265-279.

Gottfried M, Pauli H, Futschik A *et al.* (2012) Continent-wide response of mountain vegetation to climate change. *Nature Climate Change*, **2**, 111-115.

Hadfield JD (2010) MCMC methods for multi-response generalized linear mixed models: the MCMCglmm R package. *Journal of Statistical Software,* **33**, 1-22.

Hodgson JA, Thomas CD, Oliver TH, Anderson BJ, Brereton TM, Crone EE (2011) Predicting insect phenology across space and time. *Global Change Biology*, **17**, 1289-1300.

Huete A, Didan K, Miura T, Rodriguez EP, Gao X, Ferreira LG (2002) Overview of the radiometric and biophysical performance of the MODIS vegetation indices. *Remote Sensing of Environment,* **83**, 195-213.

Inouye DW, Morales MA, Dodge GJ (2002) Variation in timing and abundance of flowering by *Delphinium barbeyi* Huth (Ranunculaceae): the roles of snowpack, frost, and La Niña, in the context of climate change. *Oecologia,* **130**, 543-550.

Jackson G, Crocker C, Barnard J, Gradwell G, Edwardes S, Jackson M, Bloomer J (2012) Database of British and Irish Hills v12. http://hills-database.co.uk/database_notes.html.

Johns TC, Gregory JM, Ingram WJ *et al.* (2003) Anthropogenic climate change for 1860 to 2100 simulated with the HadCM3 model under updated emissions scenarios. *Climate Dynamics,* **20**, 583-612.

Keeling CD, Chin JFS, Whorf TP (1996) Increased activity of northern vegetation inferred from atmospheric CO_2 measurements. *Nature,* **382**, 146-149.

Körner C (2003) *Alpine plant life: functional plant ecology of high mountain ecosystems,* Berlin, Germany, Springer Verlag.

Menzel A, Sparks TH, Estrella N *et al.* (2006) European phenological response to climate change matches the warming pattern. *Global Change Biology,* **12**, 1969-1976.

Miller-Rushing AJ, Høye TT, Inouye DW, Post E (2010) The effects of phenological mismatches on demography. *Philosophical Transactions of the Royal Society B: Biological Sciences,* **365**, 3177-3186.

Morin X, Viner D, Chuine I (2008) Tree species range shifts at a continental scale: new predictive insights from a process-based model. *Journal of Ecology,* **96**, 784-794.

NASA Land Processes Distributed Active Archive Center (2013) MOD13Q1: Vegetation Indices 16-Day L3 Global 250m. USGS/Earth Resources Observation and Science (EROS) Center, Sioux Falls, South Dakota.

Pauli H, Gottfried M, Dullinger S *et al.* (2012) Recent plant diversity changes on Europe's mountain summits. *Science,* **336**, 353-355.

Pettorelli N, Vik JO, Mysterud A, Gaillard J-M, Tucker CJ, Stenseth NC (2005) Using the satellite-derived NDVI to assess ecological responses to environmental change. *Trends in Ecology & Evolution,* **20**, 503-510.

Phillimore AB, Stålhandske S, Smithers RJ, Bernard R (2012) Dissecting the contributions of plasticity and local adaptation to the phenology of a butterfly and its host plants. *The American Naturalist,* **180**, 655-670.

Post ES, Pedersen C, Wilmers CC, Forchhammer MC (2008) Phenological sequences reveal aggregate life history response to climatic warming. *Ecology,* **89**, 363-370.

Qiu B, Zhong M, Zeng C, Tang Z, Chen C (2012) Effect of topography and accessibility on vegetation dynamic pattern in Mountain-hill Region. *Journal of Mountain Science,* **9**, 879-890.

Saavedra F, Inouye DW, Price MV, Harte J (2003) Changes in flowering and abundance of *Delphinium nuttallianum* (Ranunculaceae) in response to a subalpine climate warming experiment. *Global Change Biology,* **9**, 885-894.

Stöckli R, Vidale PL (2004) European plant phenology and climate as seen in a 20-year AVHRR land-surface parameter dataset. *International Journal of Remote Sensing,* **25**, 3303-3330.

Thackeray SJ, Sparks TH, Frederiksen M *et al.* (2010) Trophic level asynchrony in rates of phenological change for marine, freshwater and terrestrial environments. *Global Change Biology,* **16**, 3304-3313.

Totland Ø, Alatalo JM (2002) Effects of temperature and date of snowmelt on growth, reproduction, and flowering phenology in the arctic/alpine herb, *Ranunculus glacialis*. *Oecologia*, **133**, 168-175.

University of East Anglia Climatic Research Unit (2012) CRU Time Series (TS) high resolution gridded datasets. NCAS British Atmospheric Data Centre http://badc.nerc.ac.uk/home/.

Walther G-R, Post E, Convey P *et al.* (2002) Ecological responses to recent climate change. *Nature*, **416**, 389-395.

Wipf S, Rixen C (2010) A review of snow manipulation experiments in Arctic and alpine tundra ecosystems. *Polar Research*, **29**, 95-109.

Wood SN (2003) Thin plate regression splines. *Journal of the Royal Statistical Society: Series B (Statistical Methodology)*, **65**, 95-114.

Wu X, Liu H (2012) Consistent shifts in spring vegetation green-up date across temperate biomes in China, 1982–2006. *Global Change Biology*, 870-880.

Zhang X, Friedl MA, Schaaf CB *et al.* (2003) Monitoring vegetation phenology using MODIS. *Remote Sensing of Environment*, **84**, 471-475.

Supporting Information legends

Table S1. Full details of the Bayesian GLMMs for NDVI and EVI in each month.

Figure S1. Equivalent of Fig. 5 but for alternative temperature averaging periods.

Figure S2. Equivalent of Fig. 6 but for SRES emissions scenario A2a.

Figure S3. Equivalent of Fig. 6 but for SRES emissions scenario B2.

Figure S4. Within-summit responses to between-year temperature variation.

Figures

Figure 1. Map with points showing the locations of summits ≥600 m in elevation in Scotland. The inset histogram shows the distribution of their elevations. The map is superimposed with the 0.5° monthly temperature grid.

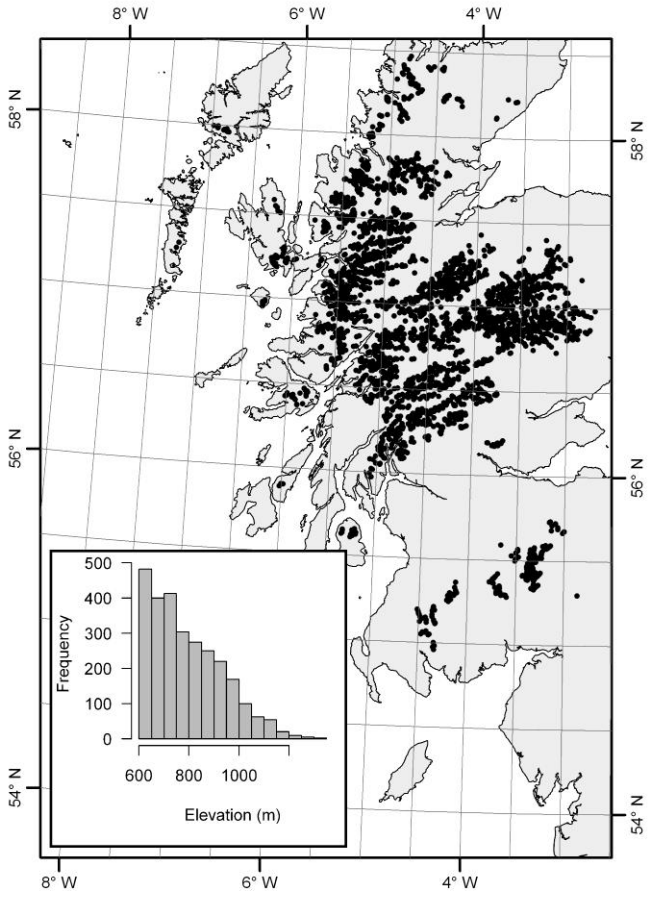

Figure 2. Data pre-processing and temporal interpolation of NDVI for an example mountain – Sgiath Chuil East Top (883 m elevation). (a) Part of the raw time series showing the distinction between observations of land, cloud and snow. (b) After exclusion of cloud and snow, outliers from the average seasonal trend were identified and removed using a circular regression spline to represent seasonal variation. The lines show three iterations of the outlier exclusion algorithm, indicating that the two iterations used in the full analysis were sufficient (negligible difference between iterations 2 and 3). (c) The time series after cloud, snow and outliers are removed. The solid line is the fitted regression spline from which first-of-month NDVI estimates were interpolated. Grey vertical lines mark occasions when observations were close enough to the first day of the month to allow interpolation. (d) Boxplot showing the interpolated first-of-month NDVI values across all years (boxes show median and interquartile range, whiskers span the range [Q_1-1.5(Q_3-Q_1), Q_3+1.5(Q_3-Q_1)], where Q_1 and Q_3 are the first and third quartiles, and points show data outside that range). Some months are missing due to lack of interpolated data from that summit.

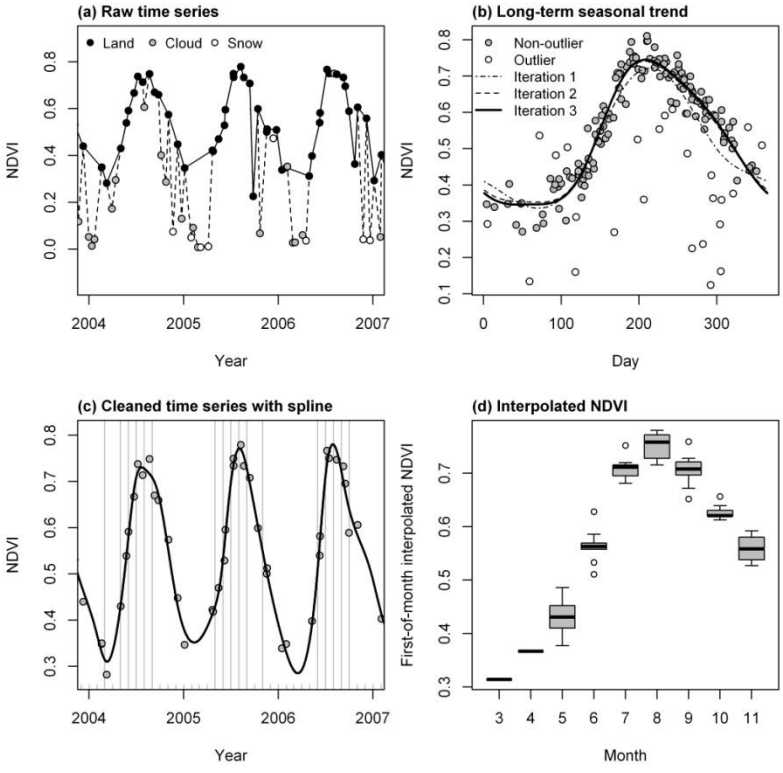

Figure 3. Median seasonal (a) NDVI and (b) EVI curves for summits in different elevational ranges, estimated from seasonal splines fitted to each summit after outlier exclusion ('Fit 3' in Fig. 2b). Points mark the median VI peak day. Internal *x*-axis ticks show the monthly division of the year.

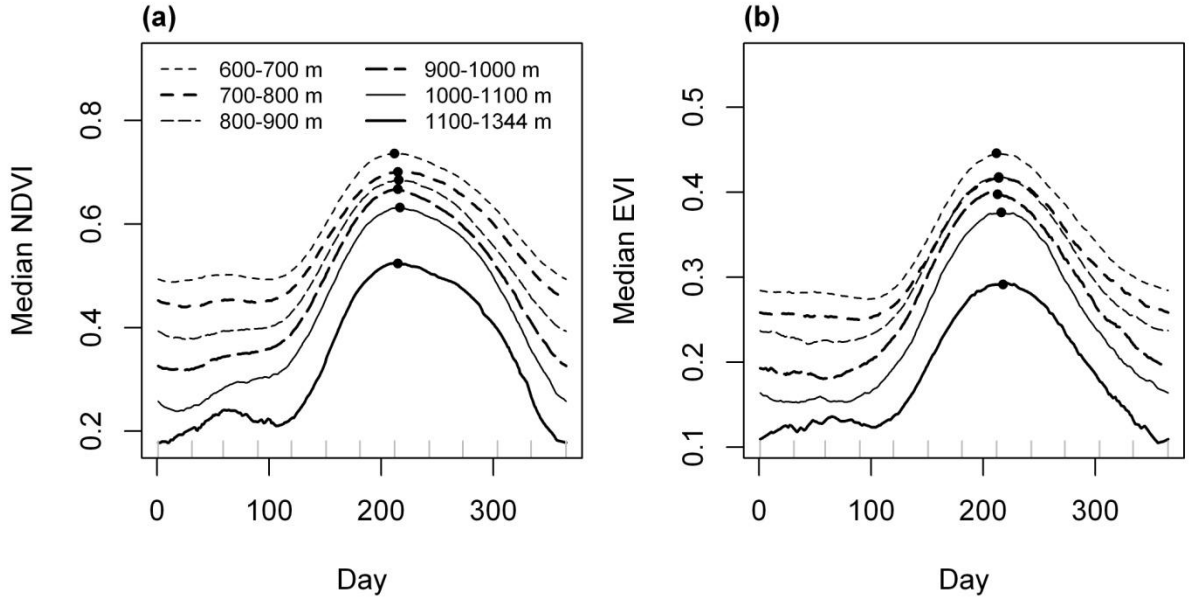

Figure 4. Sample sizes for the analysis of interpolated first-of-month NDVI for each month and 50 m elevation bins, after pre-processing (Fig. 2). Shading and contours indicate the number of interpolated values obtained. EVI showed a very similar pattern, but with slightly higher sample sizes.

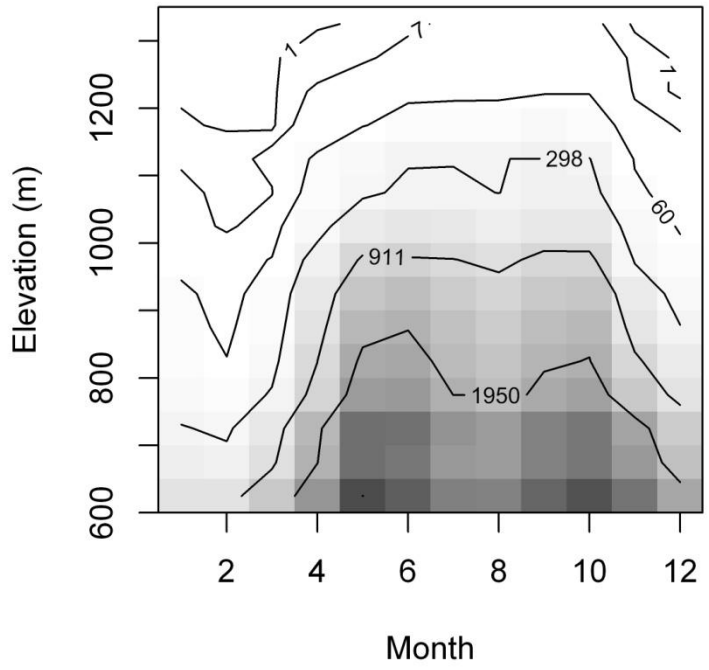

Figure 5. The estimated temperature sensitivity of interpolated first-of-month (a) NDVI and (b) EVI at different elevations and months. Shading and contours indicate the expected change in VI for a 1 °C increase in the mean temperature of the previous three months, as estimated from the posterior means of the Bayesian GLMMs. Asterisks label months in which the posterior distributions indicated a statistically significant interaction between elevation and temperature ($P < 0.05$).

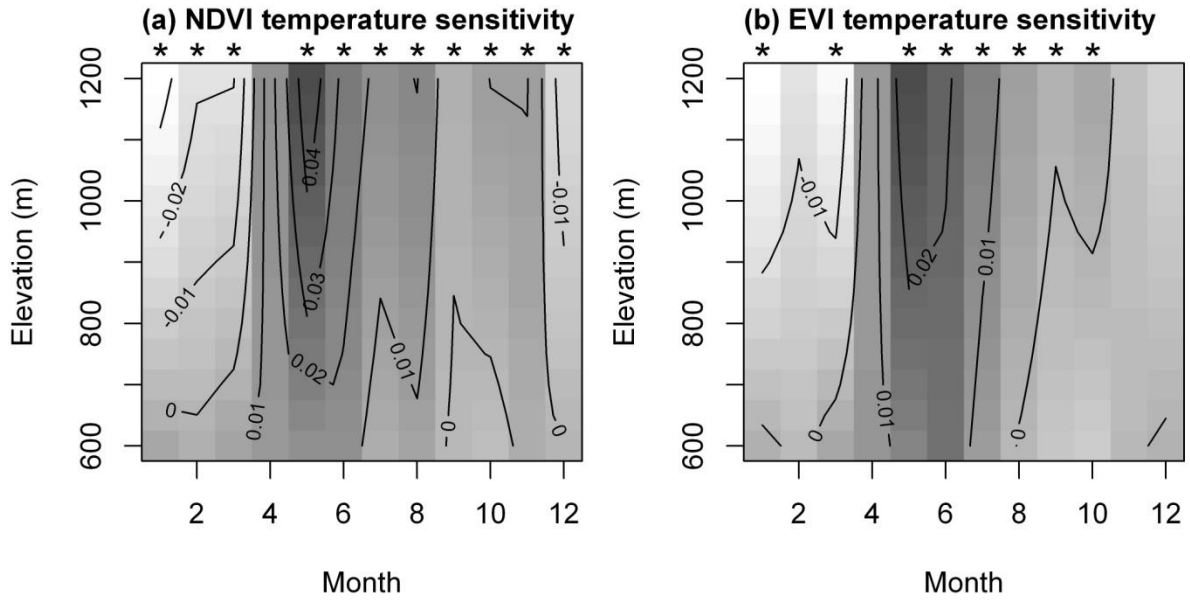

Figure 6. Expected change in first-of-month (a-b) NDVI and (c-d) EVI caused by warming up to the 2050s predicted under SRES scenario A1b by the HadCM3 climate model. Black lines and symbols show the median VIs predicted for the 2050s, according to the modelled temperature-sensitivities (Fig. 5). In the left-hand panel, grey lines show median fitted VI values for summits grouped by elevation over the current day period of study. For comparability, VIs for both periods are calculated from posterior mean fixed effects only. In (b) and (d), barplots show the median predicted regional warming in the previous three months (secondary axis). The small difference between barplots is due to the different subsets of valid data used in the analyses of NDVI and EVI.

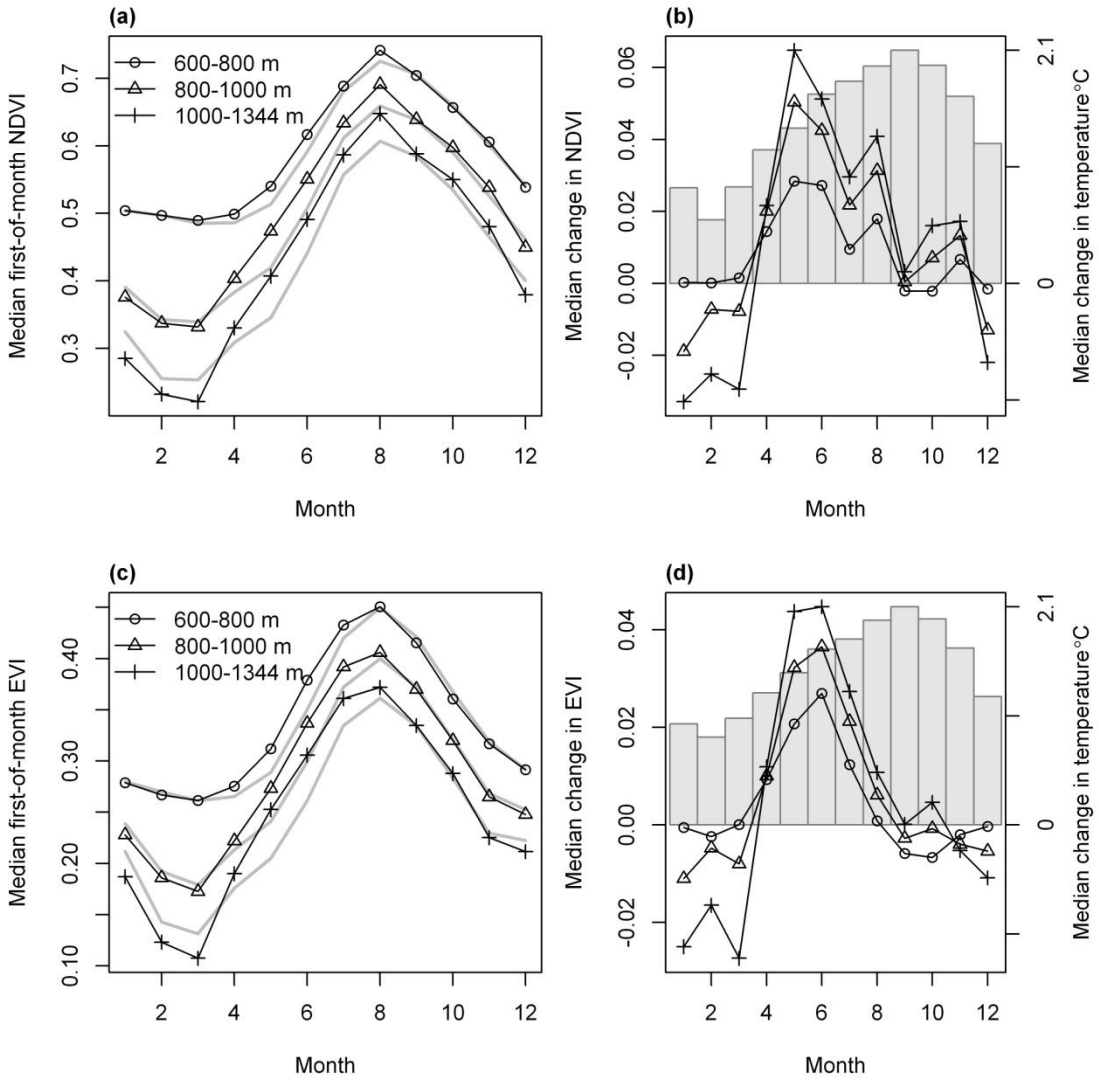

Supporting Information

Table S1. Fixed effects from the Bayesian GLMMs fitted to first-of-month vegetation indices in each calendar month (sample sizes given), given as the posterior means, 95% highest posterior density intervals (HPD) and two-tailed *P* values estimated from $5x10^5$ MCMC iterations.

Vegetation index	Month	Fixed effect	Posterior mean	95% HPD	*P*
NDVI	1 (n=2083)	Intercept	1.263	0.241-2.269	0.015
		log_{10}-Elevation	-0.269	-0.623-0.095	0.138
		Temperature	0.372	0.177-0.560	<0.001
		Temperature x log_{10}-Elevation	-0.132	-0.198--0.063	<0.001
	2 (n=1621)	Intercept	3.184	2.562-3.816	<0.001
		log_{10}-Elevation	-0.955	-1.175--0.733	<0.001
		Temperature	0.224	0.070-0.377	0.004
		Temperature x log_{10}-Elevation	-0.080	-0.132--0.024	0.004
	3 (n=3613)	Intercept	3.270	2.945-3.613	<0.001
		log_{10}-Elevation	-0.991	-1.111--0.876	<0.001
		Temperature	0.268	0.155-0.379	<0.001
		Temperature x log_{10}-Elevation	-0.094	-0.134--0.055	<0.001
	4 (n=10396)	Intercept	3.014	2.809-3.222	<0.001
		log_{10}-Elevation	-0.907	-0.979--0.835	<0.001
		Temperature	-0.020	-0.084-0.043	0.544
		Temperature x log_{10}-Elevation	0.012	-0.011-0.034	0.307
	5 (n=21351)	Intercept	3.749	3.596-3.898	<0.001
		log_{10}-Elevation	-1.174	-1.226--1.122	<0.001
		Temperature	-0.271	-0.297--0.245	<0.001
		Temperature x log_{10}-Elevation	0.103	0.094-0.112	<0.001
	6 (n=21821)	Intercept	3.015	2.819-3.210	<0.001
		log_{10}-Elevation	-0.894	-0.962--0.827	<0.001
		Temperature	-0.084	-0.113--0.057	<0.001
		Temperature x log_{10}-Elevation	0.036	0.027-0.046	<0.001
	7 (n=17202)	Intercept	3.355	3.012-3.691	<0.001
		log_{10}-Elevation	-0.962	-1.084--0.849	<0.001
		Temperature	-0.115	-0.152--0.077	<0.001
		Temperature x log_{10}-Elevation	0.043	0.030-0.056	<0.001
	8 (n=15552)	Intercept	3.455	3.019-3.917	<0.001
		log_{10}-Elevation	-1.003	-1.166--0.855	<0.001
		Temperature	-0.108	-0.147--0.069	<0.001
		Temperature x log_{10}-Elevation	0.042	0.028-0.055	<0.001
	9 (n=19679)	Intercept	3.011	2.631-3.359	<0.001
		log_{10}-Elevation	-0.807	-0.927--0.676	<0.001
		Temperature	-0.042	-0.069--0.014	0.002
		Temperature x log_{10}-Elevation	0.014	0.005-0.024	0.004
	10 (n=21134)	Intercept	4.198	3.803-4.600	<0.001
		log_{10}-Elevation	-1.240	-1.377--1.101	<0.001
		Temperature	-0.143	-0.174--0.112	<0.001
		Temperature x log_{10}-Elevation	0.050	0.039-0.060	<0.001
	11 (n=12386)	Intercept	3.235	2.506-3.951	<0.001
		log_{10}-Elevation	-0.947	-1.196--0.691	<0.001
		Temperature	-0.067	-0.135-0.003	0.052
		Temperature x log_{10}-Elevation	0.025	0.001-0.049	0.034

Vegetation index	Month	Fixed effect	Posterior mean	95% HPD	*P*
	12 (n=7041)	Intercept	1.533	0.801-2.304	<0.001
		log_{10}-Elevation	-0.344	-0.614--0.084	0.011
		Temperature	0.152	0.057-0.249	0.002
		Temperature x log10-Elevation	-0.055	-0.088--0.021	0.002
EVI	1 (n=2612)	Intercept	0.326	-0.555-1.277	0.484
		log_{10}-Elevation	-0.013	-0.350-0.296	0.930
		Temperature	0.195	0.023-0.369	0.026
		Temperature x log_{10}-Elevation	-0.070	-0.130--0.008	0.024
	2 (n=2738)	Intercept	1.889	1.487-2.315	<0.001
		log_{10}-Elevation	-0.570	-0.721--0.429	<0.001
		Temperature	0.091	-0.018-0.191	0.087
		Temperature x log_{10}-Elevation	-0.033	-0.068-0.005	0.080
	3 (n=5663)	Intercept	1.803	1.577-2.010	<0.001
		log_{10}-Elevation	-0.546	-0.618--0.466	<0.001
		Temperature	0.199	0.126-0.274	<0.001
		Temperature x log_{10}-Elevation	-0.070	-0.096--0.044	<0.001
	4 (n=12600)	Intercept	1.477	1.332-1.603	<0.001
		log_{10}-Elevation	-0.436	-0.480--0.385	<0.001
		Temperature	0.014	-0.031-0.058	0.553
		Temperature x log_{10}-Elevation	-0.002	-0.017-0.014	0.783
	5 (n=23777)	Intercept	1.843	1.729-1.951	<0.001
		log_{10}-Elevation	-0.570	-0.607--0.531	<0.001
		Temperature	-0.123	-0.142--0.101	<0.001
		Temperature x log_{10}-Elevation	0.049	0.041-0.055	<0.001
	6 (n=23521)	Intercept	1.541	1.370-1.713	<0.001
		log_{10}-Elevation	-0.458	-0.517--0.398	<0.001
		Temperature	-0.021	-0.046-0.002	0.080
		Temperature x log_{10}-Elevation	0.014	0.006-0.022	<0.001
	7 (n=17880)	Intercept	2.077	1.769-2.410	<0.001
		log_{10}-Elevation	-0.608	-0.723--0.501	<0.001
		Temperature	-0.062	-0.095--0.024	0.002
		Temperature x log_{10}-Elevation	0.024	0.012-0.037	<0.001
	8 (n=15747)	Intercept	2.352	1.889-2.808	<0.001
		log_{10}-Elevation	-0.673	-0.826--0.509	<0.001
		Temperature	-0.057	-0.096--0.017	0.004
		Temperature x log_{10}-Elevation	0.020	0.006-0.034	0.003
	9 (n=18930)	Intercept	2.375	1.977-2.757	<0.001
		log_{10}-Elevation	-0.674	-0.805--0.536	<0.001
		Temperature	-0.052	-0.084--0.024	0.001
		Temperature x log_{10}-Elevation	0.017	0.007-0.028	0.002
	10 (n=20005)	Intercept	2.810	2.389-3.235	<0.001
		log_{10}-Elevation	-0.843	-0.991--0.699	<0.001
		Temperature	-0.097	-0.130--0.063	<0.001
		Temperature x log_{10}-Elevation	0.033	0.021-0.044	<0.001
	11 (n=12023)	Intercept	1.478	0.694-2.187	<0.001
		log_{10}-Elevation	-0.404	-0.651--0.127	0.002
		Temperature	0.018	-0.054-0.089	0.632
		Temperature x log_{10}-Elevation	-0.007	-0.032-0.018	0.603
	12 (n=7267)	Intercept	0.762	0.026-1.473	0.044
		log_{10}-Elevation	-0.164	-0.422-0.087	0.200
		Temperature	0.078	-0.014-0.171	0.100
		Temperature x log_{10}-Elevation	-0.028	-0.059-0.006	0.096

Figure S1. Equivalent of Fig. 5 but for alternative temperature averaging periods (left-hand labels).

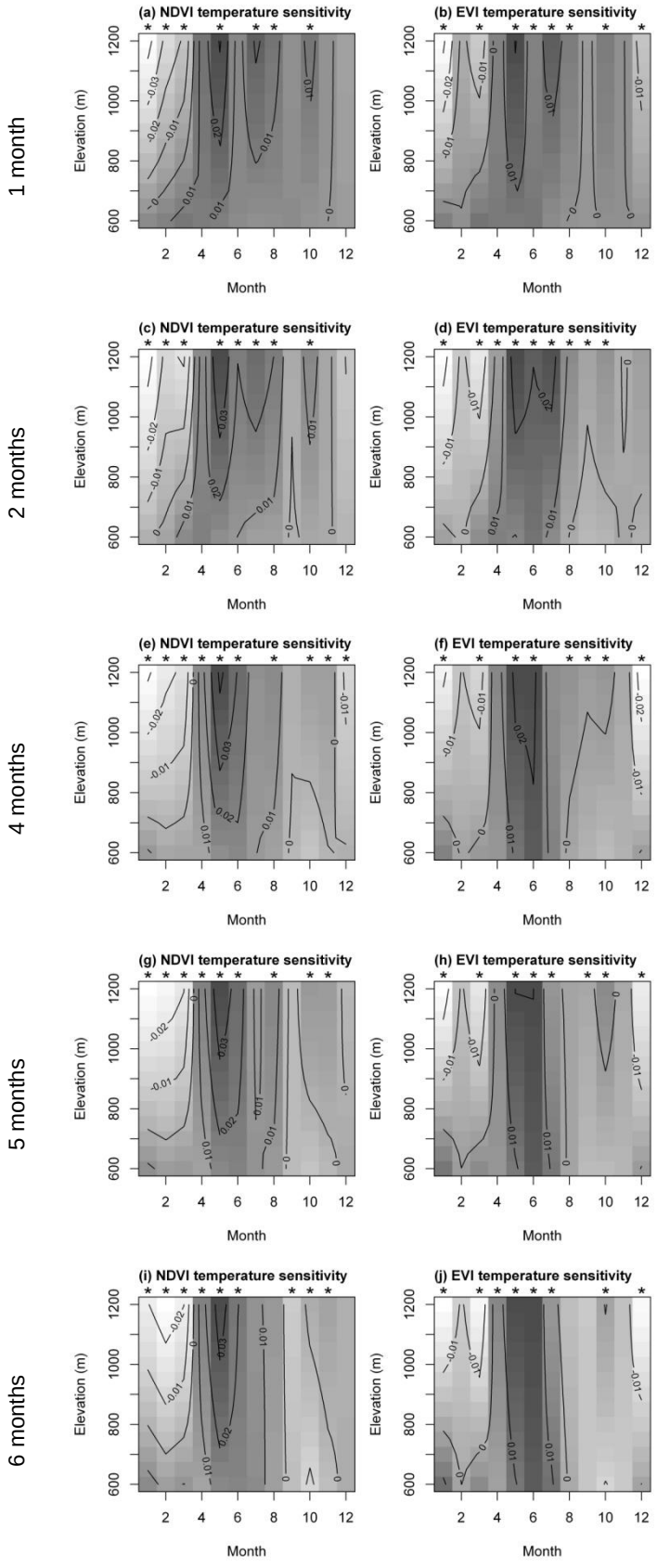

Figure S2. Equivalent of Fig. 6 but for SRES emissions scenario A2a.

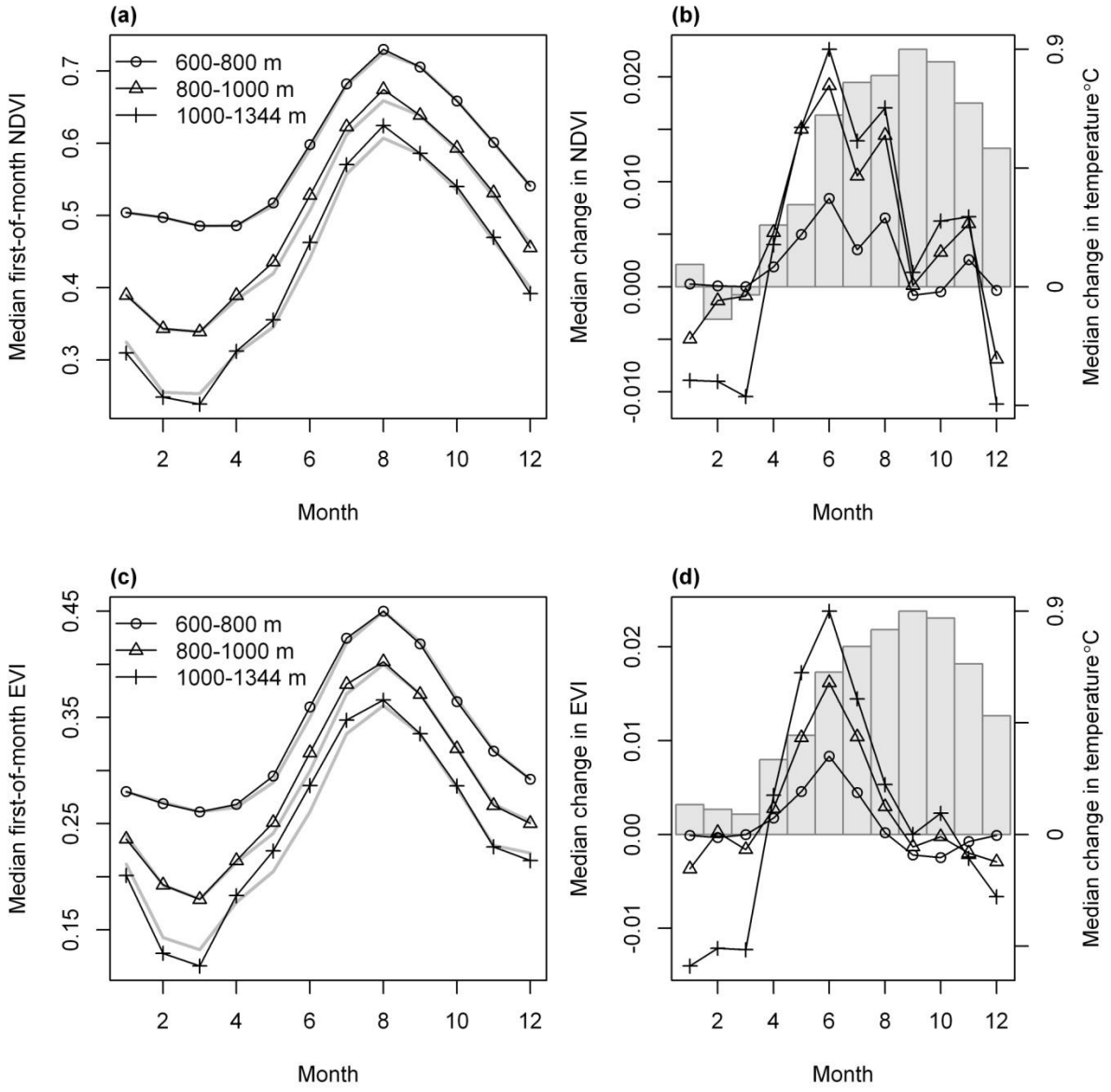

Figure S3. Equivalent of Fig. 6 but for SRES emissions scenario B2.

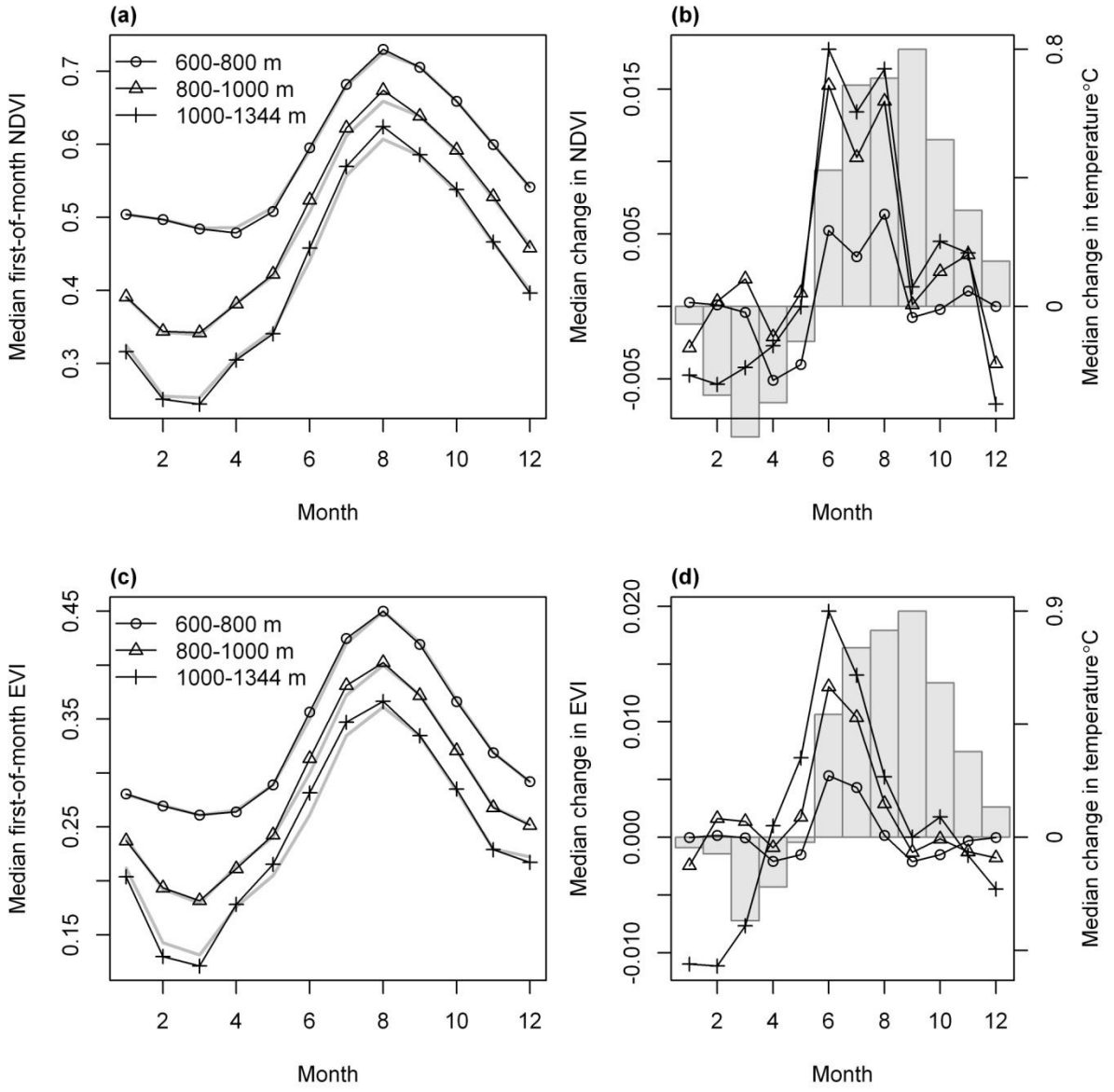

Figure S4. Within-summit responses to between-year temperature variation. Plots show median within-summit Pearson's correlation coefficients between temperature in the previous three months and first-of-month (a) NDVI and (b) EVI for groups of mountains at different elevations. Correlations were only calculated for summit-month combinations with at least six interpolated VI values, so values are missing where no summits met this requirement. The strong positive correlations in spring show that local vegetation activity varied in response to between-year variation in temperature.